

Experimental investigation of the unsteady response of premixed flame fronts to acoustic pressure waves

Athéna Wangher, Geoff Searby*, and Joël Quinard

CNRS and Aix-Marseille Université
Institut de Recherche sur les Phénomènes Hors Équilibre
49 rue Frédéric Joliot-Curie
F-13384 MARSEILLE cedex 13, France
Revised version, January 2008.

Abstract

Using OH* chemiluminescence, we measure the experimental unsteady response of a 1-D premixed flame to an acoustic pressure wave for a range of frequencies below and above the inverse of the flame transit time. We find that the response is positive and, at low frequency the order of magnitude is comparable with existing theoretical analyses. However, if it is supposed that the chemiluminescence is proportional to the mass consumption rate, despite some uncertainty in the interpretation of the chemiluminescence signal we find that the frequency dependence of the measured response is *not* compatible with the predictions of the standard flame model for one-step Arrhenius kinetics. A better, but not perfect, correlation is obtained for the heat release rate. We conclude that the standard model does not provide an adequate description of the unsteady response of real flames, and that it is necessary to investigate more realistic chemical models.

Key words: Acoustic-flame interaction, Combustion instabilities, Instantaneous reaction rate, Chemiluminescence

1. Nomenclature

1.1. Dimensioned quantities

c	Speed of sound	m s^{-1}
m	Mass consumption rate	$\text{kg m}^{-2} \text{s}^{-1}$
p	Acoustic pressure	Pa
u	Acoustic velocity	m s^{-1}
k	Acoustic wavenumber	m^{-1}
E_A	Activation energy	J
I	Luminous intensity	Arbitrary units
R	Gas constant	$\text{J mole}^{-1} \text{K}^{-1}$
T	Temperature	K
U_L	Laminar flame velocity	m s^{-1}
D_{th}	Thermal diffusivity	$\text{m}^2 \text{s}^{-1}$
D_{mol}	Molecular diffusivity	$\text{m}^2 \text{s}^{-1}$
\dot{Q}	Heat release rate	$\text{J m}^{-2} \text{s}^{-1}$

δ	Flame thickness, D_{th}/U_L	m
τ_t	Flame transit time, δ/U_L	s
ω	Angular frequency	s^{-1}
ρ	Density	kg m^{-3}

1.2. Non-dimensional quantities

β	Zeldovich number	$E_A(T_b - T_o)/RT_b^2$
γ	Ratio of specific heats	C_p/C_v
Le	Lewis number	D_{th}/D_{mol}

1.3. Subscripts

o	Fresh gas
b	Burnt gas

2. Introduction

The presence of thermo-acoustic instabilities is a long-standing problem in practical combustion de-

* Corresponding author
Email address: Geoff.Searby@irphe.univ-mrs.fr (Geoff Searby).

vices [1–5]. The basic physics of thermo-acoustic instabilities are well known: Rayleigh in 1878 [6] showed that an acoustic wave is amplified if fluctuations of the heat release rate are locally in phase with the oscillations of acoustic pressure. If the presence of the acoustic wave can modulate the heat release from the combustion zone, then the system is potentially unstable. There are many possible mechanisms by which an acoustic wave can influence combustion, and the dominant mechanism will vary with the design of the combustion device. Possible coupling mechanisms include:

- a) periodic oscillations of the equivalence ratio, particularly when the fuel is injected as a liquid [7–9],
- b) oscillations of total flame area induced by convective effects [10, 11],
- c) oscillations of flame area induced by the acoustic accelerations [12–15] and
- d) direct sensitivity of the chemical reaction rate to the local pressure [16–21]

A review of the relative strengths of mechanisms *a*, *c* and *d*, in a particularly simple 1-D configuration has been performed by Clanet et al. [22].

Existing theoretical analyses of direct effect of pressure oscillations on the mass consumption rate and on the reaction rate, mechanism *d*, [17, 19] have never been validated experimentally. The purpose of this paper is to report experimental observations of the strength and phase of the instantaneous chemiluminescence from premixed planar methane and propane flames subjected to a pure pressure oscillation over a wide range of frequencies of the order of the inverse of the flame transit time.

3. Theoretical background

If a chemical reaction is governed by an Arrhenius-type law, then it is obvious that the reaction rate will be sensitive to pressure, both through the density pre-factor, and also through the exponential sensitivity to the temperature. The linearised response of a 1-D premixed flame to high frequency pressure oscillations has been calculated analytically by Clavin *et al.* [17] and by McIntosh [19–21]. Both authors have supposed that the chemistry is governed by a one-step Arrhenius law with a high activation energy. The gas expansion ratio is not restricted.

Clavin *et al.* present a calculation in the distinguished limit $\beta(Le - 1) \approx 1$, where β is the reduced activation energy $\beta = E_A(T_b - T_o)/RT_b^2$, supposed to be large, and Le is the Lewis number, $Le = D_{th}/D_{mol}$, supposed to be close to unity. The analysis is limited to moderate frequencies such that the acoustic period can be shorter than the flame transit time, τ_t , but the acoustic wavelength is much greater

than the flame thickness. The result of Clavin *et al.* for the unsteady part of the mass consumption rate can be written in a dimensional form as :

$$\frac{m'/\rho U_L}{p'/\rho c^2} = \frac{E_A}{RT_b}(\gamma - 1) \frac{A(\omega)}{B(\omega)} i\omega\tau_t \quad (1)$$

with

$$A(\omega) = \{q - (T_b - T_o)/T_b\} q \quad (2)$$

$$B(\omega) = \{q - 1\} q^2 - \frac{\beta}{2}(Le - 1) \{1 - q + 2i\omega\tau_t\} \quad (3)$$

$$q(\omega) = \{1 + 4i\omega\tau_t\}^{\frac{1}{2}} \quad (4)$$

McIntosh has also calculated the flame response function [19, 21] using similar approximations. He has further extended his analysis to ultra high frequencies where the flame thickness is comparable to the acoustic wavelength [20, 23]. His ultra high frequency result is given as a non linear partial differential equation which can be solved only numerically. However, in this present study, we will not be concerned with the very high frequency behaviour.

McIntosh and Clavin use slightly different mathematical techniques to linearise their equations, and their results are formally different. However, numerical evaluations using realistic parameter values yield results that are quite similar. The result of McIntosh [19] can be written in a dimensional form as follows :

$$\frac{m'/\rho U_L}{p'/\rho c^2} = \frac{E_A}{RT_b}(\gamma - 1) \frac{A'(\omega)}{B'(\omega)} i\omega\tau_t \quad (5)$$

with

$$A'(\omega) = \{r - (T_b - T_o)/T_b\} \quad (6)$$

$$B'(\omega) = \{q - 1\} r + \frac{\beta}{2} \left\{ 1 - q - \frac{(1 - r)}{Le} \right\} \quad (7)$$

$$q(\omega) = \{1 + 4i\omega\tau_t\}^{\frac{1}{2}} \quad (8)$$

$$r(\omega) = \{1 + 4i\omega\tau_t Le\}^{\frac{1}{2}} \quad (9)$$

Note that, in his papers, McIntosh uses a definition of the Lewis number which is the inverse of that used here.

The amplitude and phase of these analytical response functions are plotted in figures 1 and 2 as a function of the logarithm of the reduced frequency, $\omega\tau_t$, for three Lewis numbers, using a typical activation energy for hydrocarbon flames, $E_A/RT_b = 10.5$ and a burnt gas temperature, $T_b = 1800$ K representative of our experiments.

The numerical evaluations of the analyses of Clavin and of McIntosh yield results that are similar. The low and high frequency limits of both

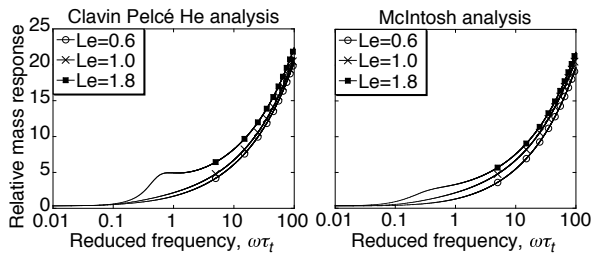


Fig. 1. Semi-log plots of the dimensionless ratio of mass flux to pressure oscillation as a function of dimensionless frequency for three Lewis numbers.

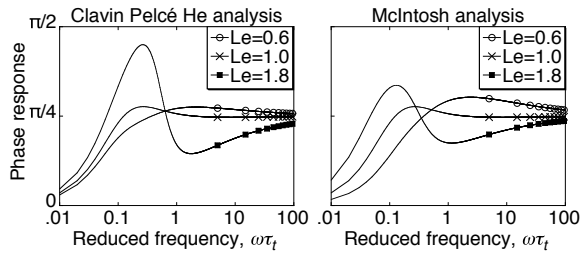


Fig. 2. Semi-log plots of phase response against dimensionless frequency for three Lewis numbers.

analyses are identical, both for the amplitude of the response function, and for the phase of the response. When the frequency is close to the inverse of the flame transit time, there is a weak resonance, which increases in strength as the Lewis number increases. This resonance is slightly stronger according to the analysis of Clavin. In the case of unit Lewis number, the expression given by Clavin and by McIntosh become identical. There is also a corresponding oscillation in the phase of the response, which goes from zero phase difference in the low frequency limit, to $\pi/4$ in the high frequency limit.

The general tendency of the amplitude of the response function is to increase as the square root of frequency (this is not immediately apparent in the semi-log plots). Thus, although the response of this mechanism is relatively weak in the low frequency regime, $\omega\tau_t \ll 1$, it increases continuously with frequency. According to McIntosh's numerical results [21], the response function is further enhanced in the high frequency regime before reaching a broad maximum at a reduced frequency of the order $\omega\tau_t \approx (E_a/RT_b)^2 \approx 100$. In terms of real frequency, this is of the order of 100 kHz for typical hydrocarbon-air flames. This turn-over frequency is much higher than the frequencies found in industrial thermo-acoustic instabilities, and is beyond the range of the experiments presented here.

These analytical predictions for the 1-D response of premixed flames to an acoustic perturbation have never been validated experimentally. We attempt to do this in the experiments described below. Premixed flames of methane and propane are main-

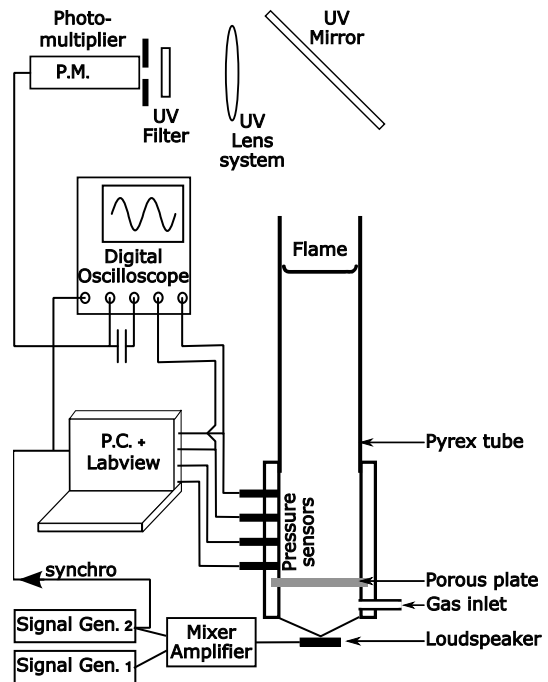


Fig. 3. Experimental set-up.

tained perfectly planar using a periodic acceleration field [14, 24]. The flames are then subjected to a periodic pressure fluctuation at a different higher frequency. The unsteady response of the flame is monitored using the spontaneous ultra-violet emission of the hydroxyl radical, OH^* , at 307 nm. It will be seen that the experimental response of the flame does *not* increase with frequency.

4. Experimental apparatus

The experimental set-up is shown in figure 3. The initial flows of fuel (methane or propane) and oxidant (air) were regulated using sonic nozzles. The combustible mixture was produced in excess at a constant rate. Part of the mixture was fed to the main burner and the excess mixture was consumed in a secondary burner. By this means the flow rate in the main burner could be altered continuously without any danger of changing the composition of the mixture.

The main burner consisted essentially of a half-open Pyrex tube, fed with the combustible mixture at the closed end. A porous plate made of sintered brass was placed just above the gas entry to laminarise the flow. In order to cover a wide range of frequencies, two tubes were used. For the high frequency domain, the tube was 600 mm long with an internal diameter of 45 mm. For the low frequency domain the tube was 3 150 mm long with an internal diameter of 95 mm. These diameters were chosen to

minimise acoustic losses. The tube was excited simultaneously at two different resonant frequencies using a loudspeaker placed at the closed end of the tube. A flexible cooling pipe was wrapped around the Pyrex tube just ahead of the flame front in order to suppress radiative and conductive heating of the upstream burner walls.

4.1. Flame stabilisation and excitation

4.1.1. Stabilisation

The flame could be positioned anywhere in the tube and was maintained perfectly stationary in the laboratory frame by carefully adjusting the gas flow rate. The tube was systematically excited at the lowest, quarter-wavelength, acoustic mode. The flame was placed in the downstream region of the tube and was thus subjected to this periodic acoustic velocity field which served to suppress the Darrieus-Landau cellular instability and produce a perfectly flat 1-D flame [14, 24]. This acoustic re-stabilisation occurs when the amplitude of the acoustic velocity oscillation is of the order of 4 times the laminar burning velocity, and also if the burning velocity is below a critical limit. For lean methane and propane flames, the fastest flames that could be stabilised this way were 190 mm/s and 210 mm/s respectively. The corresponding flame thickness and transit times were in the range $100 \leq \delta \leq 180 \mu\text{m}$ and $0.5 \leq \tau_t \leq 2.0 \text{ms}$ respectively. For faster flames, a secondary parametric instability appears on the flame front before the acoustic level is sufficient to suppress the Darrieus-Landau instability [14].

4.1.2. Excitation

The tube was then excited at a higher resonant frequency, typically the third to fifth overtones, and the flame was positioned at exactly the last pressure anti-node of this excitation frequency. The position of this pressure antinode was calculated in real time from measurements of the acoustic field (see below) and the flame was brought to, and held at this position by small manual adjustments of the gas flow rate. We then monitored the response of the flame to this excitation frequency. The reduced frequency $\omega\tau_t$ was varied continuously, within a limited range, by changing the laminar burning speed. It was also changed discontinuously both by changing the excited overtone, and by changing the tube length.

4.2. Determination of the acoustic field

We found that a single acoustic sensor was not sufficient to characterise the amplitude and phase of

the acoustic fields. At the quarter-wavelength resonant frequency, the acoustic field is described, to a reasonable approximation, by a quarter-wavelength with a velocity node at the closed end and a pressure node at the open end. However for higher overtones, the end-correction ($\approx 0.6 R$) for the apparent position of the pressure node at the open end is no longer negligible compared to the wavelength. Moreover the presence of the flame and the associated jump in sound speed between the fresh and burnt gases introduces a phase jump in the acoustic field at the flame front, so the position of the velocity node with respect to the loudspeaker was also poorly determined. For all these reasons, it was necessary to monitor the acoustic field using four acoustic sensors in the upstream field, separated by approximately $1/16$ of the acoustic wavelength at the excitation frequency. We suppose that the standing wave in the upstream region of burner can be described by the sum of two counter-propagating waves. The first wave propagates away from the loudspeaker and is described by an amplitude A and a phase ϕ_0 . The second wave resulting from the reflections at the flame front and at the tube exit propagates towards the loudspeaker and is described by an amplitude B and a phase $\phi_0 + \Delta\phi$:

$$p'(x, t) = A \sin(\omega t - kx + \phi_0) + B \sin(\omega t + kx + \phi_0 + \Delta\phi). \quad (10)$$

This equation contains three unknowns A, B and $\Delta\phi$. The phase ϕ_0 corresponds to the origin of time and is irrelevant. Using three measurements of the time averaged r.m.s. values of the pressure, \hat{p}'_{x_i} , made at three positions in the tube, x_{1-3} , it is possible to calculate the values of A, B and $\Delta\phi$ and thus reconstruct the envelope of the standing wave in the upstream flow. A fourth redundant measurement provides a means to check the calculation, and also a means to eliminate false solutions when the pressure amplitudes at two sensors are almost equal.

$$\Delta\phi = \tan^{-1} \left(\frac{c(\hat{p}'_1^2 - \hat{p}'_2^2) - a(\hat{p}'_1^2 - \hat{p}'_3^2)}{d(\hat{p}'_1^2 - \hat{p}'_2^2) - b(\hat{p}'_1^2 - \hat{p}'_3^2)} \right) \quad (11)$$

$$a = \cos(2kx_1) - \cos(2kx_2)$$

$$b = \sin(2kx_1) - \sin(2kx_2)$$

$$c = \cos(2kx_1) - \cos(2kx_3)$$

$$d = \sin(2kx_1) - \sin(2kx_3)$$

$$A^2, B^2 = \frac{v \pm \sqrt{(v^2 - 4w)}}{2} \quad (12)$$

$$v = \hat{p}_3^2 - \frac{(\hat{p}_1^2 - \hat{p}_2^2) \cos(2kx_3 + \Delta\phi)}{\cos(2kx_1 + \Delta\phi) - \cos(2kx_2 + \Delta\phi)}$$

$$w = \left(\frac{(\hat{p}_1^2 - \hat{p}_2^2)}{2(\cos(2kx_1 + \Delta\phi) - \cos(2kx_2 + \Delta\phi))} \right)^2$$

The signal corresponding to pressure oscillations from the low acoustic frequency used for flame stabilisation were eliminated by Fourier filtering of time slices of the signal. A program written under Labview calculated these quantities in real time, and provided the operator with the positions and amplitude of the pressure anti-nodes. It should be remarked that these quantities change with the position of the flame in the tube and also with the temperature of the burnt gases, so that positioning the flame at a pressure anti-node is an iterative process that is almost impossible to resolve in advance.

4.3. Monitoring the unsteady flame response

The unsteady flame response was monitored using the UV emission at 307 nm from the excited OH* radical produced in the reaction zone. It is widely supposed that the production rate of OH* radicals, and thus the strength of OH* emission, is proportional to chemical reaction rate, particularly in lean flames [25–32]. It may be remarked that the flames are perfectly planar, so the measured intensities are intensity per unit area. In our experiments the OH* emission is monitored through the burnt gas, as shown in figure 3. A UV-mirror is placed downstream from the tube exit. A pair of quartz lenses form an image of the central region of the flame front on a diaphragm. The light then passes through an UV interference filter centred at 307 ± 8 nm and is detected on a photomultiplier (Hamamatsu R750). As a check, a few measurements were also made using the visible emission from the CH* radical.

At low frequencies, the normalised response of the flame, $(m'/\rho U_L) / (p'/\rho c^2)$ is predicted to be of order unity. The maximum amplitude of pressure oscillation in the tube was of order 140 dB or 200 Pa at high frequency, increasing to 155 dB, or 1100 Pa, at low frequency. So the relative fluctuation in the luminous emission was expected to be of the order of $2 \cdot 10^{-3}$ to 10^{-2} , which is weak. In order to improve the signal to noise ratio, the unsteady signal was time-averaged using a digital oscilloscope triggered by the acoustic signal generator. One channel was used to record the DC level and a second channel was used to record the fluctuating component. A third channel was used to record the acoustic pressure from one of the pressure sensors. This latter provided a means to obtain the phase delay between

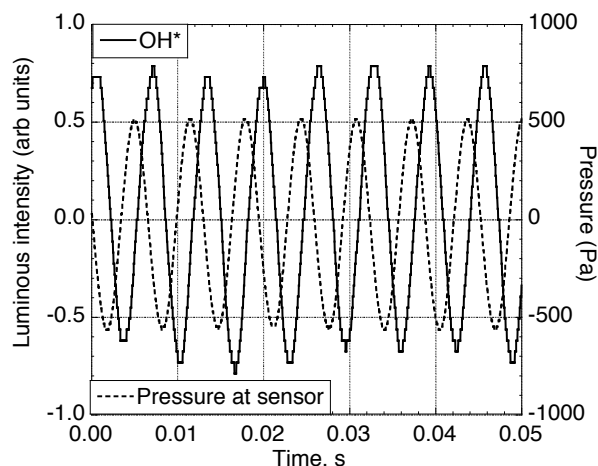


Fig. 4. A time-averaged OH* and pressure signals showing the response of a 0.15 m/s methane flame to a pressure modulation at 155 Hz and 1050 Pa.

the acoustic pressure and the flame response. Averaged OH* and pressure signals are shown in figure 4. The pressure at the sensor is not the pressure at the flame front.

5. Results

In figures 5 and 6 we plot the relative response of lean methane and propane flames respectively as a function of the reduced frequency, $\omega\tau_t$. The response function plotted here is

$$\frac{I'/\bar{I}}{p'/(p c^2)} \frac{RT_b}{E_A} \frac{1}{\gamma - 1} \quad (13)$$

where I' is the amplitude of oscillation of the OH* emission at the excitation frequency, \bar{I} is the mean intensity of OH* emission, and p' is the amplitude of pressure oscillation at the flame front. If the intensity of spontaneous emission from the OH* radical, is proportional to the instantaneous mass consumption rate of the flame, the ratio I'/\bar{I} can be compared with the calculated mass flux ratio m'/\bar{m} . We have divided both sides of eq. (1) by $(\gamma - 1)E_A/RT_b$ so that the main effect of changing the equivalence ratio and the burnt gas temperature should be normalised out of the experimental data. The activation energy was taken as 156.7 kJ/mole for lean methane flames and 123.6 kJ/mole for lean propane flames. The burnt gas temperature was calculated at each equivalence ratio using the GASEQ utility provided by Chris Morley [33]. We have also plotted the theoretical value of the response using eq. (1) for two values of the Lewis number that cover the experimental value. The theoretical values calculated using eq. (5) are not significantly different (not shown).

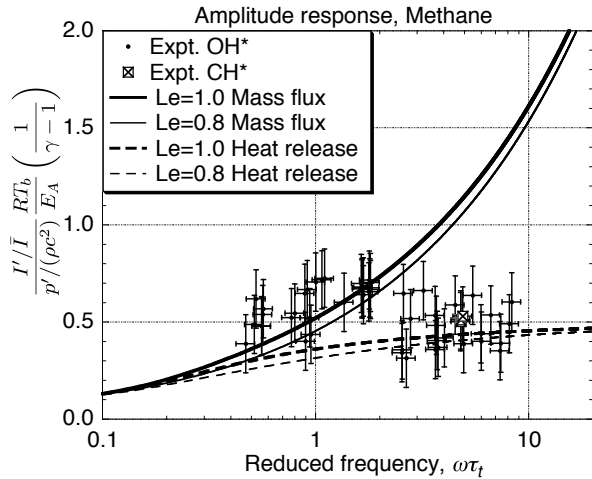


Fig. 5. Amplitude response of a planar methane flame to pressure oscillations as a function of reduced frequency. Small dots: OH* emission. Open squares: CH* emission. Full lines: Mass flux response. Dotted lines: Heat release response.

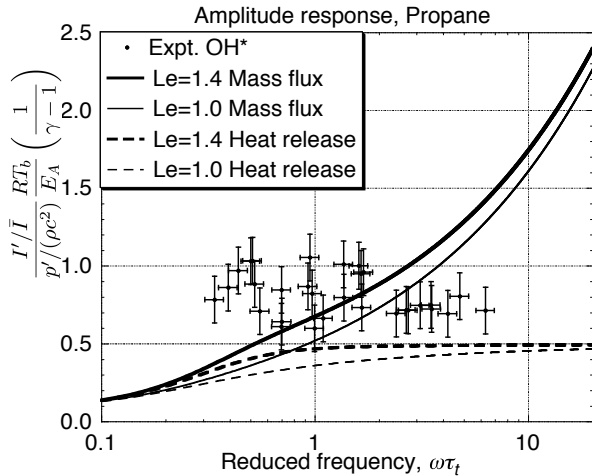


Fig. 6. Amplitude response of a planar propane flame to a pressure oscillation as a function of reduced frequency. Full lines: Mass flux response. Dotted lines: Heat release response.

There is a considerable scatter of the experimental points. The main origin of the scatter is experimental uncertainty, since we measure a small oscillation whose relative amplitude is $\approx 10^{-3}$ on a relatively weak and noisy signal. The reduced frequency is in the range $0.4 < \omega\tau_t < 9$, corresponding to real frequencies in the range $90 \text{ Hz} < f < 1000 \text{ Hz}$. Nevertheless it is obvious that the experimental points do not follow the theoretical curves for the mass flux.

As a check, in figure 5 we have also plotted a few points obtained from measurements of the excited CH* radical in the methane flame. These points lie well within the spread of the OH* measurements and confirm that our results are not sensitive to the particular species used to monitor the flame response.

For both methane and propane fuels, the experimental amplitude response is independent

of frequency to within experimental uncertainty. For methane we find a reduced response equal to 0.5 ± 0.2 , and for propane we find a reduced response equal to 0.8 ± 0.25 . Over the same frequency range, the theoretical response curves increase by a factor five. We have verified the relation between the steady-state OH* emission and the steady mass consumption rate for variation of the equivalence ratio and for variation of the fresh gas temperature [34]. The relationship was found to be linear, but with a zero offset. For the sake of simplicity we have not applied the correction stemming from this work. If we were to do so, it would scale the experimental points in figs 5 and 6 downwards by about 50%, bringing the low frequency experimental points into closer agreement with the analytical prediction. However, such a correction would only increase the difference between experiment and theory at high frequency. Our experimental measurements are thus not compatible with the theoretical predictions for the unsteady mass consumption rate.

Due to unsteady effects inside the preheat zone, there is a difference between the unsteady mass consumption rate and the unsteady heat release rate. Assuming that the heat release rate is proportional to the temperature gradient evaluated on the cold side of the reaction zone, this latter can be evaluated from eq. (4.8) of ref.[17]. We find the following response function for the heat release rate, \dot{Q}' :

$$\frac{\dot{Q}'/\bar{Q}}{p'/\rho c^2} = \frac{E_A}{RT_b}(\gamma - 1) \frac{(q - 1)}{2} \frac{A(\omega)}{B(\omega)} \quad (14)$$

where, A , B and q are given by eqs.(2), (3) and (4) respectively.

This heat release response function is also plotted in figures 5 and 6. It can be seen that the amplitude of the measured OH* emission is in better agreement with the theoretical unsteady heat release rate than with the mass consumption, especially at high frequency.

Figures 7 and 8 show the measured phase of the response of the methane and propane flames. For both fuels we find that the phase of response decreases as the reduced frequency increases. We have also plotted the theoretical phase response of the mass flux predicted by eq. (1) and the heat flux eq. (14). Again, our experimental values are closer to the theoretical predictions for heat release rate than for the mass flux, although the observed amplitude of variation is larger than the theoretical prediction, particularly for methane flames. At the highest frequency attainable, it is not certain that we have reached a limiting value for the phase, but the experimental points suggest that the asymptote is close to zero, in fair

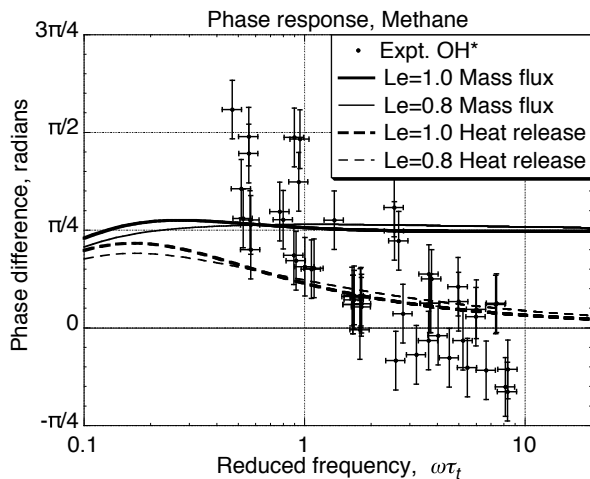


Fig. 7. Phase response of a planar methane flame to a pressure oscillation as a function of reduced frequency. Full lines: Mass flux response. Dotted lines: Heat release response.

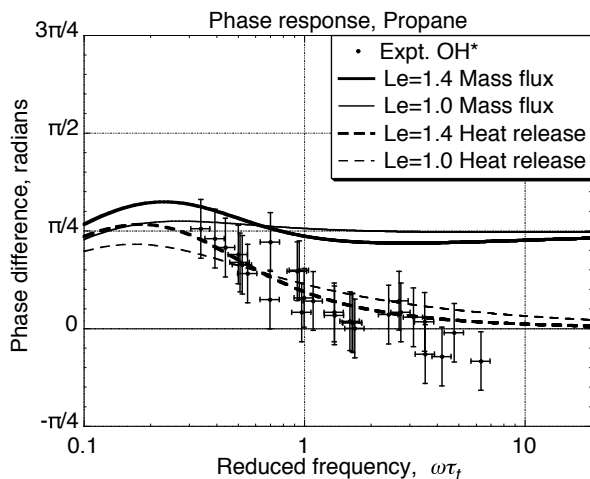


Fig. 8. Phase response of a planar propane flame to a pressure oscillation as a function of reduced frequency. Full lines: Mass flux response. Dotted lines: Heat release response.

agreement with the predictions for the heat release rate.

6. Discussion and conclusions

Despite the rather large experimental uncertainties, and also some uncertainty in the interpretation of the chemiluminescence signal, we first remark that the presence of an acoustic wave does indeed have a measurable effect on the unsteady chemiluminescence, and thus presumably on the unsteady reaction rate. The response is always positive and, at low frequencies, the order of magnitude is compatible with predicted response of both the mass consumption rate and the heat release rate, indicating that this mechanism can contribute to the gain of thermo-acoustic instabilities.

Nevertheless, the frequency dependence of our experimental data is *not* compatible with the theoretical predictions for the unsteady mass burning rate of standard asymptotic flame theory based on the assumption of a high activation energy with one step Arrhenius chemical kinetics. The theory predicts that the unsteady 1-D response of a premixed flame to pressure oscillations should increase as the square root of frequency, our measurements find a response that is independent of frequency over more than a decade. The agreement is better with the theoretical prediction for the unsteady heat release rate.

This simple (although delicate) fundamental experiment shows that the luminous flame emission is better correlated to unsteady heat release than to unsteady mass consumption rate. The order of magnitude is correct but the quantitative agreement is not excellent. There are two possible reasons for these differences:

- (i) The OH* chemiluminescence is not a good measure of the unsteady response of the flame.
- (ii) The unsteady response of multi-step chemical kinetics to pressure is qualitatively different to that of one step Arrhenius kinetics.

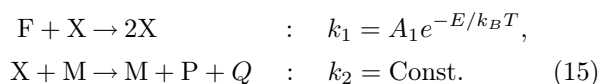
These two reasons are not necessarily exclusive. However we can reasonably eliminate the third possibility of an error in the theoretical analysis, since two independent authors, using slightly different mathematical approximations and techniques, predict an almost identical unsteady response for one-step kinetics.

It is known that OH* chemiluminescence is a decreasing function of pressure, through collisional quenching [30]. This means that, in presence of an acoustic wave, the proportionality constant relating the relative chemiluminescence fluctuation, I'/I , to the relative mass flux fluctuation, m'/\bar{m} , will be smaller than unity, contrary to our assumption in section 5. However, since collisional quenching is a very fast process, it will not introduce any frequency dependence on the acoustic time scales. So, in the frame of one step kinetics, the effect of pressure on collisional quenching will be only to renormalise the experimental points in figures 5 and 6, it cannot change the frequency dependence.

Using 2-D numerical simulations with detailed chemical kinetics, Najm and co-workers [35] already remarked that chemiluminescence is not a good tracer of the unsteady heat release of very highly strained flames in interaction with a strong vortex pair. They attribute this decorrelation to effects of multi-step chemical kinetics.

The above remarks lead us to conclude that the main reason for disagreement between our experimental results and standard flame theory lies in the

over-simplifying assumption of one-step Arrhenius kinetics in the latter. In order to provide further understanding, it is necessary to investigate the unsteady pressure response of a more realistic chemical kinetic model. As a first step, an analytical investigation of the response of a simple two-step reaction has been performed in this laboratory by Clavin and Searby [36]. They have considered an irreversible chain-branching step and an irreversible completion or chain breaking reaction:



In the first temperature dependent auto-catalytic reaction, an intermediate species, X, attacks a reactant species, F, to produce more intermediate species. In the second step, a completion reaction converts the intermediate species, X, into products P and heat Q by collision with any species M. For simplicity, the first reaction is treated as non-exothermic. This model is even simpler than the Liñan-Zelovich two-step reaction [37, 38], in that the chain-breaking is here treated as a first order reaction.

The first results of this two step model confirm that multi-step chemical kinetics substantially modify the amplitude and frequency dependence of the unsteady pressure response of premixed flames, in particular at high frequencies, $\omega\tau_t > 1$. This suggests that it is worthwhile pursuing investigations of the unsteady response of multi-step chemical kinetics.

Acknowledgements

This work was performed as part of the French ANR project number BLAN07-2-182685. We wish to thank Jacky Minelli for his help in the construction of the experiment. We also thank Axelle Amon and Rémi Arnaud for their help in setting up the experiment, and Paul Clavin for helpful discussions.

References

- [1] L. Crocco, S. Cheng, Theory of combustion instability in liquid propellant rocket motors, Butterworths, London, 1956.
- [2] D. Harrje, F. Reardon, Tech. Rep. SP-194, NASA, Washington, DC (1972).
- [3] F. Culick, in: Combustion instabilities in liquid fuelled propulsion systems, Vol. N° 450 of AGARD Conference proceedings, NATO, 1988, pp. 1.1–1.73.
- [4] V. Yang, A. Anderson, Liquid rocket engine combustion instability, Vol. 169 of Progress in Astronautics and Aeronautics, AIAA, Washington DC, 1995.
- [5] W. Krebs, P. Flohr, B. Prade, S. Hoffmann, Combustion Science and Technology 174 (2002) 99–128.
- [6] J. Rayleigh, Nature 18 (1878) 319–321.
- [7] P. Clavin, J. Sun, Combustion Science and Technology 78 (1991) 265–288.
- [8] J. Buckmaster, P. Clavin, Proceedings of the Combustion Institute 24 (1992) 29–36.
- [9] T. Lieuwen, Y. Neumeier, B. Zinn, Combustion Science and Technology 135 (1998) 193–211.
- [10] T. Poinso, A. Trounev, D. Veynante, S. Candel, E. Esposito, Journal of Fluid Mechanics 177 (1987) 265–292.
- [11] D. Durox, T. Schuller, S. Candel, Proceedings of the Combustion Institute 29 (2002) 69–75.
- [12] A. Putnam, R. Williams, Proceedings of the Combustion Institute 4 (1952) 556–575.
- [13] G. Markstein, in: Proc. Sixth Natl. Congr. Appl. Mech., Cambridge, Mass, 1970, pp. 11–33.
- [14] G. Searby, D. Rochwerger, Journal of Fluid Mechanics 231 (1991) 529–543.
- [15] P. Pelcé, D. Rochwerger, Journal of Fluid Mechanics 239 (1992) 293–307.
- [16] R. Dunlap, Tech. Rep. Project MX833, Report UMM-43, Aeronautical Research Center. University of Michigan (1950).
- [17] P. Clavin, P. Pelcé, L. He, Journal of Fluid Mechanics 216 (1990) 299–322.
- [18] G. Ledder, A. K. Kapila, Combustion Science and Technology 76 (1991) 21–44.
- [19] A. McIntosh, Combustion Science and Technology 75 (1991) 287–309.
- [20] A. McIntosh, Combustion Science and Technology 91 (1993) 329–346.
- [21] A. McIntosh, Philosophical Transactions of the Royal Society of London A 357 (1999) 3523–3538.
- [22] C. Clanet, G. Searby, P. Clavin, Journal of Fluid Mechanics 385 (1999) 157–197.
- [23] G. Batley, A. McIntosh, J. Brindley, Combustion Science and Technology 92 (1993) 367–388.
- [24] C. Clanet, G. Searby, Physical Review Letters 80 (17) (1998) 3867–3870.
- [25] D. Stepowski, A. Cessou, P. Goix, Combustion and Flame 99 (1994) 516–522.
- [26] J. Kojima, Y. Ikeda, T. Nakajima, Proceedings of the Combustion Institute 28 (2000) 1757–1764.
- [27] K. T. Walsh, M. B. Long, M. Tanoff, M. D. Smooke, Proceedings of the Combustion Institute 27 (1998) 615–623.

- [28] J. Luque, J. B. Jeffries, G. P. Smith, D. R. Crosley, K. T. Walsh, M. B. Long, M. D. Smooke, *Combustion and Flame* 122 (2000) 172–175.
- [29] B. Higgins, M. McQuay, F. Lacas, J. Rolon, N. Darabiha, S. Candel, *Fuel* 80 (2001) 67–74.
- [30] N. Docquier, S. Belhalfaoui, F. Lacas, N. Darabiha, C. Rolon, *Proceedings of the Combustion Institute* 28 (2002) 1765–1774.
- [31] Y. Hardalupas, M. Orain, *Combustion and Flame* 139 (2004) 188–207.
- [32] R. Balachandran, B. Ayoola, C. Kaminski, A. Dowling, E. Mastorakos, *Combustion and Flame* 143 (2005) 37–55.
- [33] C. Morley.
URL <http://www.gaseq.co.uk/>
- [34] A. Wangher, J. Quinard, G. Searby, in: I. Gökalp (Ed.), *European Combustion Meeting 2007, Crête, Vol. on CD ROM, The Combustion Institute, 2007*, p. 6 pages.
URL <http://hal.archives-ouvertes.fr/hal-00161753>
- [35] H. N. Najm, P. H. Paul, C. J. Mueller, P. S. Wyckoff, *Combustion and Flame* 113 (1998) 312–332.
- [36] P. Clavin, G. Searby, *Combustion Theory and Modelling* To appear.
- [37] Y. Zel'dovich, *Kinetika i Katalis* 2 (1961) 305–313.
- [38] A. Liñan, Afosr contract no. e00ar68-0031, INTA Madrid (1971).